

# Force-based Heterogeneous Traffic Simulation for Autonomous Vehicle Testing

Qianwen Chao<sup>1,2</sup>, Xiaogang Jin<sup>3</sup>, Hen-Wei Huang<sup>4</sup>, Shaohui Foong<sup>2</sup>, Lap-Fai Yu<sup>5</sup>, and Sai-Kit Yeung<sup>6</sup>

**Abstract**—Recent failures in real-world self-driving tests have suggested a paradigm shift from directly learning in real-world roads to building a high-fidelity driving simulator as an alternative, effective, and safe tool to handle intricate traffic environments in urban areas. To date, traffic simulation can construct virtual urban environments with various weather conditions, day and night, and traffic control for autonomous vehicle testing. However, mutual interactions between autonomous vehicles and pedestrians are rarely modeled in existing simulators. Besides vehicles and pedestrians, the usage of personal mobility devices is increasing in congested cities as an alternative to the traditional transport system. A simulator that considers all potential road-users in a realistic urban environment is urgently desired. In this work, we propose a novel, extensible, and microscopic method to build heterogeneous traffic simulation using the *force-based* concept. This force-based approach can accurately replicate the sophisticated behaviors of various road users and their interactions through a simple and unified way. Furthermore, we validate our approach through simulation experiments and comparisons to the popular simulators currently used for research and development of autonomous vehicles.

## 1. INTRODUCTION

Autonomous vehicles have the potential to improve the quality and productivity of the time spent on cars during a trip, increase the safety and efficiency of the transportation system, and transform transportation into a utility available to anyone, anytime. Recent advances in the field of perception [1], planning [2], [3], and decision-making [4] for autonomous vehicles have led to implementation of several prototypes already being tested on roads. Although the development of a variety of machine learning approaches largely facilitate the decision making and planning through learning from the interactions between autonomous vehicles and real world environments [5]–[7], the limited amount of real-world data, which can barely support the complex traffic scenarios, constrain autonomous driving systems in learning diverse driving strategies. These make the unmanned vehicles always adopt the most conservative and inefficient decisions for safety reasons. Despite this, it has been reported that these autonomous vehicles have caused some fatal accidents in the real world. Handling the complex interactions with other road users in various traffic scenarios remains a great challenge in autonomous driving [8].

<sup>1</sup>Department of Computer Science, Xidian University, chaoqianwen15@gmail.com

<sup>2</sup>The Engineering Product Development, Singapore University of Technology and Design.

<sup>3</sup>State Key Lab of CAD&CG, Zhejiang University.

<sup>4</sup>Koch Institute, Massachusetts Institute of Technology.

<sup>5</sup>Computer Science Department, George Mason University.

<sup>6</sup>The Division of Integrative Systems and Design, Hong Kong University of Science and Technology.



Fig. 1. Example mixed traffic simulation result generated by our approach.

Due to the past failure cases of autonomous vehicles in real world, a high-fidelity driving simulator has become an alternative and effective tool to provide various kinds of traffic conditions for motion control of autonomous vehicles, allowing for safety tests before real-world road driving [9]–[11]. Recently, the Apollo simulation platform [12] and Best et al.’s work [13] make efforts to provide powerful virtual traffic scenarios for driving strategy testing of autonomous vehicles. Both simulations implement two non-vehicle traffic participants: pedestrians and cyclists. However, the behaviors of these non-vehicle road users have been pre-defined and cannot react to vehicle motions in real time. Besides, an open-source simulator, Carla [14], has been developed to support the development, training, and validation of autonomous urban driving systems, which offers flexible specification of sensor suites and various environmental conditions. Although dynamic pedestrians are introduced into the simulation, the interaction between vehicle and pedestrian is handled in a simple predefined way: in an interaction, the pedestrian stops to wait for a few seconds as sensing any vehicles, then walks anyway without considering the existence of the vehicle. From this point of view, current existing simulators merely make decisions of autonomous vehicles motion in a reactive way without considering any mutual influences and real interactions between vehicles and other potential road-users. As bicycle usage and pedestrian walking have been increasing in many countries in urban areas due to potential environmental and health benefits, creating a mixed simulation environment (Fig. 1) consisting of mutual influences and interactions among vehicles, two-wheelers, and pedestrians, is highly desired.

In this paper, we focus on modeling the heterogeneous traffic composed of various types of road-users by a unified approach that can facilitate autonomous driving strategy test-

ing. Current existing microscopic modeling methods [15]–[17] and traffic simulators (SUMO [18], SimMobility [19] and Vissim [20]) have always separately modeled the behavior of vehicles, pedestrian, bicycles and their interactions. Furthermore, each specific behavior of each types of road-user, such as vehicle acceleration and lane change, is modeled and controlled individually. Such non-unified approaches are complicated and inefficient in generating complex virtual traffic environments.

Here, we propose a simple, efficient, scalable *force-based* framework to uniformly simulate the behaviors of vehicles, pedestrians, bicycles, and the interactions among them, in which any detailed behavior for each category of individuals can be attributed to a specific force. We make three contributions:

- It introduces a novel, scalable framework based on the *force-based* concept to generate complex virtual urban traffic environments for autonomous vehicle testing.
- Unlike previous traffic simulation methods, it introduces a unified model for various detailed behaviors of vehicles, including acceleration/deceleration, lane keeping, and lane changing behavior.
- It provides a viable solution for describing the interactions among different types of road users in simulation.

Benefits of this method have been verified in experimental tests at the end of this paper.

## 2. FORCE-BASED FRAMEWORK

We present a two-layered force-based framework for hybrid traffic simulation. Specifically, the top layer calculates the detailed motions of each kind of road users respectively by interpreting them as different forms of force according to their different behavioral characteristics. In the second layer, the force-based model is extended to describe the interaction between different road users. As the simulated environment is constructed for the unmanned vehicles testing, we would mainly focus on the interactions that may influence the decision making of autonomous vehicle, which are the vehicle-pedestrian and vehicle-bicycle interactions.

Inspired by the social force model [21]–[24] for pedestrian dynamics, the participants in mixed traffic act as if they would be subjected to ‘force’ from the influences of their desire, their neighboring participants and the built environment such as road structures, walls or buildings. Specifically, assuming that individual  $i$  is an arbitrary road user in the mixed traffic flow, its motion is determined by a combination of sociopsychological and physical forces. The total effect force  $\mathbf{F}_i(t)$  is defined as follows:

$$\mathbf{F}_i(t) = \mathbf{F}_i^0(t) + \sum_{j(\neq i)} \mathbf{F}_{ij}(t) + \sum_W \mathbf{F}_{iW}(t) + \sum_o \mathbf{F}_{io}(t), \quad (1)$$

where the driving force  $\mathbf{F}_i^0(t)$  reflects the individual’s intention to move to a certain destination and with a desired speed, the repulsive force  $\mathbf{F}_{ij}(t)$  describes the effects of interactions with its neighboring individuals  $j$ ,  $\mathbf{F}_{iW}(t)$  measures the repulsive effects of the built environment  $W$ , and  $\mathbf{F}_{io}(t)$  is introduced to describe the interaction with other categories of road users.

The driving force  $\mathbf{F}_i^0(t)$  describes the individual  $i$ ’s motivation to move with an expected velocity  $\mathbf{v}_i^0(t)$  by adapting the actual velocity  $\mathbf{v}_i(t)$  within a certain relaxation time  $\tau_i$  [22]:

$$\mathbf{F}_i^0(t) = m_i \frac{\mathbf{v}_i^0(t) - \mathbf{v}_i(t)}{\tau_i} = m_i \frac{\mathbf{v}_i^0(t) - \mathbf{v}_i(t)}{\mathbf{v}_i^0(t)} \mathbf{a}_i, \quad (2)$$

where  $m_i$  is the mass of individual  $i$  and  $\mathbf{a}_i$  represents the maximum acceleration.

In our framework, the repulsive force  $\mathbf{F}_{ij}$  from a certain neighbor  $j$  is presented in different forms according to different characteristics of various kinds of road users. For a pedestrian, this force is defined as a combination of social-psychological and physical forces, describing the psychological tendency of two pedestrians to stay away from each other, and the physical contact force when the pedestrians touch each other, respectively. For vehicles, the repulsive force comes from all the neighboring vehicles within sight in the current and adjacent lanes. For a bicycle, the force is defined as a combination of the direct repulsive force for collision avoidance and the force for overtaking.

Similarly, for different types of road users, the force  $\mathbf{F}_{iW}(t)$  from the built environment is defined in different forms, depending on their specific locations and related behaviors. Specifically,  $\mathbf{F}_{iW}$  is introduced to describe pedestrian  $i$ ’s interaction with environment borders and obstacles  $W$ . For a bicycle, the repulsive force  $\mathbf{F}_{bW}$  from lane boundary  $W$  makes the bicycle  $b$  keep a certain distance from lane boundaries for safety. Analogously for vehicles,  $\mathbf{F}_{cW}(t)$  measures the repulsive force from the lane boundary  $W$ . But different from bicycles, a distinctive force  $\mathbf{F}_c^{cl}(t)$  is introduced to model vehicle behaviors in the lane-changing process.

We define the interaction force  $\mathbf{F}_{io}(t)$  as the environmental influence respectively for the interactions between vehicles and pedestrians, as well as vehicles and bicycles. The interacting individuals treat each other as the environmental influence and compute the feedback to themselves. It is worth noticing that the pedestrian behaviors are computed using the social force model. More details can be found in [21], [22].

## 3. FORCES FOR BEHAVIORS IN MIXED TRAFFIC

### 3.1. Force-based Model for Vehicles

The force-based simulation model for vehicles is designed according to the characteristics of vehicle movements:

- Drivers mainly drive in a car-following fashion. However, the vehicle’s movement is also affected by all vehicles in the field of view.
- Drivers must keep driving within the lane marks, and follow the traffic laws and regulations.
- Drivers tend to change lanes to take advantage of the allowable speed in a target lane or to cope with some imperative factors such as end of current lane.

*3.1.1) Repulsive Forces between Vehicles:* When moving along a traffic flow, a vehicle  $c$  is subjected to repulsive forces from all the neighboring vehicles within sight in its current and adjacent lanes. As illustrated in Fig. 2, due to the lane-keeping rules in traffic, the impact of the vehicle  $q$  in adjacent lanes on vehicle  $c$  is far less than that of the front vehicle  $p$  in

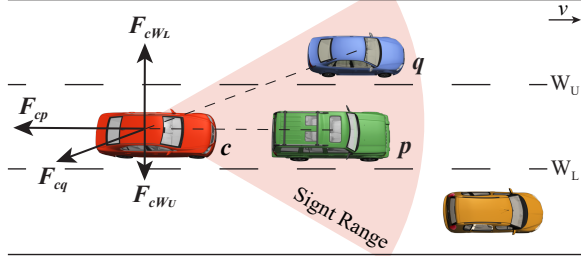


Fig. 2. The sight range (in red sector) of a vehicle  $c$  and its repulsive forces  $F_{cp}$  and  $F_{cq}$  from surrounding vehicles in the current and adjacent lanes. The repulsive forces  $F_{cW_U}$  and  $F_{cW_L}$  from two-side lane boundaries ( $W_U$  and  $W_L$ ) are also shown here.

the current lane in the absence of lane changing. Therefore, we design the repulsive force  $\mathbf{F}_{cj}$  from a certain neighbor  $j$  in different forms.

**Influence from vehicles in adjacent lanes:** The force from a neighboring vehicle  $q$  in the adjacent lane (blue vehicle in Fig. 2) is mainly associated to its distance and direction to vehicle  $c$ , defined as follows:

$$\mathbf{F}_{cq}^n(t) = U_{cq} e^{-\frac{r_{cq}}{R_{cq}}} \mathbf{n}_{cq}, \quad (3)$$

where  $U_{cq}$  is the scale factor of the repulsive force  $\mathbf{F}_{cq}^n(t)$ ,  $r_{cq}$  is the distance between the vehicle  $q$  and  $c$ ,  $R_{cq}$  is the sensitivity coefficient of the repulsive force to the distance, and  $\mathbf{n}_{cq}$  is the unit vector pointing from vehicle  $q$ 's center to vehicle  $c$ 's center.

**Influence from the vehicle in current lane:** According to the car-following phenomenon [25] in real-world traffic, vehicle  $c$ 's behavior in the current lane is mainly a response to its leading vehicle  $p$  (green vehicle in Fig. 2), for purpose of maintaining a safe gap to vehicle  $p$  while seeking for its desired velocity during driving. Here, we utilize the braking deceleration term in the popular and well-calibrated intelligent driver model (IDM) [26], [27] to approximate the repulsive force  $\mathbf{F}_{cp}^f$  of vehicle  $c$  from its leading vehicle  $p$ . Specifically, the force  $\mathbf{F}_{cp}^f$  can be defined as a function of the vehicle  $c$ 's velocity  $v_c$ , its bumper-to-bumper distance  $s$  and relative velocity  $\Delta v$  to the leading vehicle  $p$ :

$$\mathbf{F}_{cp}^f(t) = -b_c \left( \frac{s^*}{s} \right)^2 \mathbf{n}_c, \quad (4)$$

$$s^* = s_0 + v_c T_c + \frac{v_c \Delta v}{2\sqrt{a_c b_c}},$$

where the parameters  $(a_c, b_c, s_0, T_c)$  are constant for each vehicle, which describe its basic driving capability,  $a_c$  and  $b_c$  are respectively the vehicle  $c$ 's maximum acceleration and comfortable deceleration,  $s_0$  is jam space headway and  $T_c$  is the desired safety time headway,  $\mathbf{n}_c$  is the unit vector denoting the current direction of vehicle  $c$ 's movement.

**3.1.2) Force from Lane Boundaries:** The repulsive force  $\mathbf{F}_{cW}$  from two-side lane boundaries  $W$  is introduced to prompt the vehicle  $c$  to stay within the lane marks and close to the lane's central line. As shown in Fig. 2, the repulsive forces from the upper ( $W_U$ ) and lower ( $W_L$ ) boundaries of the lane, where the vehicle  $c$  is located, are respectively calculated, and their vector sum ( $\mathbf{F}_{cW_U} + \mathbf{F}_{cW_L}$ ) represents

the vehicle  $c$ 's repulsive force from all lane boundaries. When the vehicle is in the middle of the lane, the repulsive forces from  $W_U$  and  $W_L$  would compensate to each other. For each boundary  $W$ , the force is associated with the distance  $r_{cW}$  between vehicle  $c$  and lane boundary  $W$ ; that is, the closer the vehicle is to the lane boundary, the greater the repulsive force it receives. The formula of force  $\mathbf{F}_{cW}$  can be defined akin to Eq. 3.

**3.1.3) Force for Lane Changing:** A vehicle generally performs lane changing if it can go faster in a target lane. According to the lane-changing model proposed by Kesting et al. [28], the incentive condition for a lane-changing decision of the vehicle  $c$  is fulfilled if the utility of a possible lane change for vehicle  $c$  is larger than the influence on the involved neighbors (the original follower  $o$  in the original lane and the new follower  $n$  in a target lane), which is typically measured in acceleration values:

$$\tilde{a}_c - a_c + p(\tilde{a}_n - a_n + \tilde{a}_o - a_o) > \Delta a_{th}, \quad (5)$$

where the first two terms refer to the acceleration gain of a possible lane changing for vehicle  $c$  and the other terms indicate the acceleration loss of the original and new followers,  $\tilde{a}_c$  denotes the new acceleration for vehicle  $c$  after a prospective lane changing, and  $a_c$  denotes its acceleration before the lane changing. The politeness factor  $p$  determines to which degree these successors influence the lane-changing decision of vehicle  $c$ .  $\Delta a_{th}$  is the lane-changing threshold which prevents lane changes for marginal advantage [16].

If the incentive criterion (Eq. 5) is satisfied, the lane changing is performed by introducing an attraction force  $\mathbf{F}_c^{cl}$  from the target lane to vehicle  $c$ . As the attraction force is to counteract the lane-keeping constraint from current lane boundary,  $\mathbf{F}_c^{cl}$  can be computed akin to the repulsive force  $\mathbf{F}_{cW}$  from current lane boundaries, using Eq. 3.

### 3.2. Force-based Model for Bicycles

Unlike the way pedestrians and vehicles interact with their neighbors, bicyclists have their own characteristics when interacting with neighbors. First, bicycles generally do not move in a car-following manner and utilize lateral space to a greater extent than motor vehicles do. Second, unlike pedestrians, bicyclists tend to adjust their motions rather than completely stop and wait when an event happens, so as to reduce the amount of required physical exertion.

Therefore, we describe a bicycle  $k$ 's repulsive force  $\mathbf{F}_{kj}$  from its neighbor  $j$  with two force components: the direct repulsive force  $\mathbf{F}_{kj}^R$  for collision avoidance and the force  $\mathbf{F}_{kj}^E$  for overtaking:

$$\mathbf{F}_{kj}(t) = \mathbf{F}_{kj}^R(t) + \mathbf{F}_{kj}^E(t). \quad (6)$$

The direct repulsive force  $\mathbf{F}_{kj}^R$  for collision avoidance is used to describe a cyclist's conscious response to avoid collisions with other bicycles nearby. In accordance with a bicycle's shape, we use an ellipse to define a bicycle's safety space in a certain period of time, and use the semi-minor axis of the ellipse to measure the degree of other bicycles' influence. As shown in Fig. 3,  $B$  is the semi-minor axis of the ellipse and the relative velocity ( $\Delta \mathbf{v} = \mathbf{v}_k - \mathbf{v}_j$ ) of bicycle  $k$  to  $j$  lies on the semi-major axis of the ellipse. The position

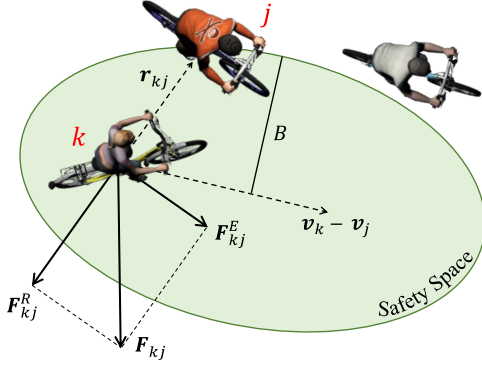


Fig. 3. Bicycle  $k$ 's repulsive forces from its neighbor bicycle  $j$ . The green ellipse area denotes the safety space of bicycle  $k$ . The bicycle  $k$ 's repulsive force  $\mathbf{F}_{kj}$  from its neighbor  $j$  can be decomposed into two force components: one direct repulsive force  $\mathbf{F}_{kj}^R$  for collision avoidance and one force  $\mathbf{F}_{kj}^E$  perpendicular to it for overtaking.

of bicycle  $k$  is the focus of the ellipse and the neighboring bicycle  $j$  is located on the circumference of the ellipse. A smaller  $B$  means shorter distance between bicycle  $k$  and  $j$ , which results in a larger repulsive force  $\mathbf{F}_{kj}^R$ . Formally, the force can be computed as follows:

$$\mathbf{F}_{kj}^R(t) = U_{kj} e^{-B/R_{kj}} \mathbf{n}_{kj}, \quad (7a)$$

$$B = \frac{1}{2} \sqrt{(\|\mathbf{r}_{kj}\| + \|\mathbf{r}_{kj} - \Delta \mathbf{v} \Delta t\|)^2 - (\|\Delta \mathbf{v} \Delta t\|)^2}, \quad (7b)$$

where  $\mathbf{r}_{kj}$  is the vector that points from bicycle  $k$  to  $j$ ,  $\Delta t$  is a time step,  $U_{kj}$  and  $R_{kj}$  are constant factors, and  $\mathbf{n}_{kj}$  is the unit vector from bicycle  $j$ 's to  $k$ .

At the same time, the overtaking force  $\mathbf{F}_{kj}^E$  is introduced to describe bicycle  $k$ 's flexible behavior when confronted with obstacles or congestion. The direction of  $\mathbf{F}_{kj}^E$  is perpendicular to the direct repulsive force  $\mathbf{F}_{kj}^R$  and the magnitude is proportional to  $\mathbf{F}_{kj}^R$ :

$$\mathbf{F}_{kj}^E(t) = \alpha \|\mathbf{F}_{kj}^R(t)\| \mathbf{n}_{kj}^V, \quad (8)$$

where  $\mathbf{n}_{kj}^V$  is the unit vector perpendicular to  $\mathbf{F}_{kj}^E$ , and  $\alpha$  is the scale factor set as 0.3 in our experiments.

### 3.3. Interactions in Mixed Traffic

In this section, we model vehicle-bicycle interactions, as well as interactions between a vehicle and a pedestrian crossing a road. In keeping with our *force-based* framework for each kind of road users, the mutual influences of the involved interacting individuals are measured in terms of forces and encoded as environmental feedbacks into their own behavioral control models.

**3.3.1) Vehicle-Bicycle Interactions:** To model vehicle-bicycle interactions, the interaction force is designed to take one of two different forms depending on the positional relationship between the bicycle  $k$  and vehicle  $c$  (see Fig. 4).

For vehicle  $c$ , if there is a side-by-side bicycle  $k$  in the sight range (the light green area), it will receive a lateral force from  $k$  for collision avoidance (Fig. 4 (a)). On the other hand, if bicycle  $k$  is traveling in the near front, vehicle  $c$  will receive a rearward force for deceleration (Fig. 4

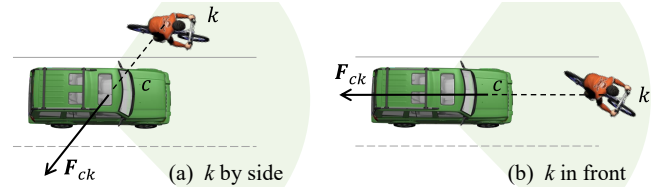


Fig. 4. Vehicle  $c$  receives repulsive force  $\mathbf{F}_{ck}$  from bicycle  $k$  in interaction.

(b)). Accordingly, the vehicle  $c$ 's interaction force  $\mathbf{F}_{ck}$  from bicycle  $k$  is defined as:

$$\mathbf{F}_{ck}(t) = \begin{cases} U_{ck} e^{-\frac{s_{ck}}{R_{ck}}} \mathbf{n}_{ck}, & k \text{ by side} \\ -b_c * \left( \frac{s_0 + v_c T_c}{s_{ck}} \right)^2 \mathbf{n}_c, & k \text{ in front} \end{cases} \quad (9)$$

where  $s_{ck}$  denotes the distance between vehicle  $c$  and bicycle  $k$ ,  $v_c$  is the velocity of the vehicle,  $\mathbf{n}_{ck}$  is the unit vector pointing from bicycle  $k$  to vehicle  $c$ , and  $\mathbf{n}_c$  represents the moving direction of vehicle  $c$ . The constant parameters ( $b_c$ ,  $T_c$ ,  $s_0$ ) describe the vehicle  $c$ 's basic driving capability, which have the same meanings as those in Eq. 4.  $U_{ck}$  and  $R_{ck}$  are constant factors.

Similarly, the interaction force  $\mathbf{F}_{kc}$  subjected on bicycle  $k$  can take one of two different forms depending on the positional relationship between  $k$  and  $c$ : whether the vehicle is by side or in front. The force is formulated akin to Eq. 9.

#### 3.3.2) Interactions with a Road-crossing Pedestrian:

When a pedestrian is about to cross a road in a mixed traffic environment, he/she perceives the surrounding traffic conditions, and the approaching vehicles correspond to his/her stimuli. Based on this perception, the pedestrian  $i$  makes a walk-or-wait decision based on gap acceptance [29], [30] to judge whether the current distance gap between him/her and the approaching vehicle  $c$  can ensure a safe crossing. Both the pedestrian's predicted crossing time  $t_i$  and the vehicle's estimated passing time  $t_c$  are computed. The crossing is considered as safe if  $t_i$  is less than  $t_c$ . Otherwise, the pedestrian needs to wait for the next longer gap.

When the pedestrian  $i$  is walking, he/she usually slows down at the beginning of crossing due to the concerns about vehicle  $c$ ' arrival time, and after successfully cutting in, the pedestrian tends to accelerate significantly due to the psychological impact of wanting to leave the danger zone. Inspired by Steven's psychophysical power law [31], we model this kind of dynamic behavior pattern and compute the interaction force  $\mathbf{F}_{ic}$  received by pedestrian  $i$  from vehicle  $c$  as follows:

$$\mathbf{F}_{ic}(t) = \beta s_{ic}^{0.67} \mathbf{n}_{ic}, \quad (10)$$

where  $s_{ic}$  is the distance between pedestrian  $i$  and vehicle  $c$  and  $\mathbf{n}_{ic}$  is the unit vector pointing from  $c$  to  $i$ .  $\beta$  is a constant scale factor set as 0.5 in our experiments.

When facing a pedestrian  $i$  trying to cross a road, vehicle  $c$  tends to decelerate for safety. This situation is similar to the sudden crossing of a bicycle as depicted in Fig. 4(b). Therefore, we calculate the interaction force  $\mathbf{F}_{ci}$  received by vehicle  $c$  from pedestrian  $i$  similarly as  $\mathbf{F}_{ck}$  in Eq. 9.

**On-line Simulation:** Up to now, each road user's detailed behavior in the mixed traffic flow has been modeled by

applying the described force-based method. Based on given initial states (position and velocity) of each road user, our method can reconstruct the sophisticated behaviors of various road users and their interactions. Taking into account the potentially complex environment required for autonomous vehicle testing, more microscopic behaviors of arbitrary road user can be easily integrated into current simulation framework by adding more specific forces.

For autonomous vehicle testing, an autonomous vehicle can be easily added into the simulation environment and controlled by its own sensing and planning algorithms. Manned vehicles, pedestrians and bicycles in the system will sense and react to the dynamic status of autonomous vehicle. It is worth mentioning that the proposed force-based approach is compatible with commercialized simulators for autonomous vehicle testing, such as Carla and Apollo. The interactions between different types of road-users in Carla and Apollo can be simply replaced with the proposed unified force approach.

#### 4. SIMULATION RESULTS

To ensure the robustness and safety of autonomous vehicles traveling on real-world roads, autonomous driving systems should be tested in virtual yet realistic traffic environments before real-world deployment. To validate our force-based simulation framework, we generate mixed traffic flow on a road without any traffic signs, which can be regarded as a complex traffic scenario for autonomous vehicle testing (Fig. 1). Table I summarizes the key parameter values used in our experiments. Note that we do not list the parameter values used in the pedestrian’s social force model, as they are set as the same as those in [22]. The parameters  $(v_c^0, a_c, b_c, s_0, T_c)$  for each vehicle are initialized by empirical values which are then added with some random perturbations to reflect individual diversity in locomotion.

TABLE I  
PARAMETER VALUES USED IN OUR EXPERIMENTS.

Parameter	Value	Unit	Description
$v_c^0$	[2,6]	$m/s$	vehicle’s optimal velocity
$a_c$	[2,3.5]	$m/s^2$	vehicle’s maximum acceleration
$b_c$	[2,3.5]	$m/s^2$	vehicle’s comfortable deceleration
$s_0$	[1.5,2.5]	$m$	jam space headway
$T_c$	[0.5,0.6]	$s$	desired safety time headway
$\Delta a_{th}$	0.5	$m/s^2$	lane changing threshold
$p$	0.4	/	politeness factor in lane changing
$U_{cq}$	3.3	/	scale factor of $F_{cq}^n$
$R_{cq}$	3.0	/	sensitivity coefficient of $F_{cq}^n$
$U_{kj}$	3.5	/	scale factor of $F_{kj}^R$
$R_{kj}$	2.0	/	sensitivity coefficient of $F_{kj}^R$
$U_{ck}$	3.5	/	scale factor of $F_{ck}$
$R_{ck}$	2.0	/	sensitivity coefficient of $F_{ck}$

As the simulated environments are constructed for unmanned vehicles testing, the following experiment results would only focus on the interactions between various vehicles, vehicles and pedestrians, as well as vehicles and bicycles, respectively. In addition, the animations of all the mentioned comparisons are shown in the supplemental video. Although the interactions between individual pedestrians, individual bicycles, as well as pedestrians and bicycles are not shown in the main results, they are all incorporated into the mixed traffic simulation.

**Timing performance:** To determine the timing performance of our force-based simulation method, we conducted a series of experiments with different numbers of individuals in the mixed traffic, in which the ratio of vehicles, bicycles and pedestrians was 1:2:3. All the timings were obtained with a 64-bit laptop machine with a 2.90 GHz Intel Core™I9-8950HK processor, 32GB memory, and an Nvidia GeForce GTX 1080 video card. The results of our performance tests shows that the computational costs scale approximately linearly with the number of road users simulated. Moreover, our approach can simulate about 800 agents in real time (30 fps) and over 1,200 agents at interactive simulation rates (10 fps). The efficient time performance indicates that our approach can be straightforwardly plugged into various existing traffic simulation systems for autonomous vehicle testing and data generation. It is noticeable that our approach is collision-free because the repelled force between each road-users significantly increases with the decrease of their distance. When the environment becomes crowded, pedestrians, bicycles and vehicles tend to keep in their lanes and reduce any interactions with each other.

**Interaction with Road-crossing Pedestrians:** We compare our force-based approach for pedestrian crossing to two popular open-source simulation platforms: Apollo [12] and Carla [14]. Fig. 5 shows the comparison results between Apollo simulation and our method. It is observed that in Apollo simulation (Fig. 5(a)), the autonomous vehicle (in blue) reacted to a pedestrian (represented as yellow rectangle) crossing the road with an initially defined constant velocity of 2.24 km/h. Since the pedestrian’s reaction to the real-time behavior of the vehicle was not considered in Apollo simulation platform, the pedestrian continued to follow the predefined path after the vehicle had completely stopped, thereby colliding with the vehicle (at the 880th frame in Fig. 5(a)). By contrast, our force-based approach attempted to mimic the real pedestrian-vehicle interaction in which both the pedestrian and vehicle made decisions based on the other one’s instantaneous status (Fig. 5(b)).

Fig. 6 shows the velocities of both the pedestrian (in yellow lines) and vehicle (in blue lines) through (a) Apollo simulation and (b) our force-based approach. It is observed in our approach that the vehicle and the pedestrian both decelerated for safety as they sensed each other. Subsequently after the vehicle completely stopped, the pedestrian accelerated to cross the lane as quickly as possible. Finally, both of them recovered to their original status after the interaction. However, in the result of Apollo simulation shown in Fig. 6 (a), the autonomous vehicle braked urgently when the pedestrian came close and the pedestrian did not react to the vehicle’s behaviors.

The Carla simulation platform models pedestrian-vehicle interactions with a simple rule-based approach: when a vehicle appears on the pedestrian’s planned route, the pedestrian momentarily stops moving. After waiting for a couple of seconds, the pedestrian will continue to walk even if there is a vehicle in front of the pedestrian.

Through the above comparisons, it is clearly shown that the force-based approach models pedestrian-vehicle interactions in a more realistic and smooth manner in the pedestrian

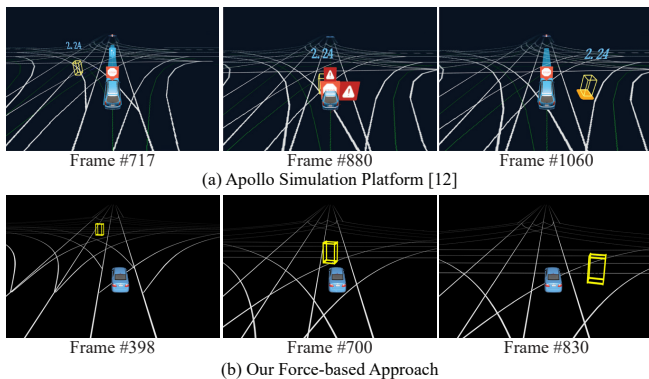


Fig. 5. Simulation results of the intersection scenario that a pedestrian (in yellow rectangle) tends to cross the road when a blue vehicle is coming, using (a) Apollo simulation platform and (b) our force-based method. The pedestrian’s movement was predefined with a constant velocity of 2.24 km/h in Apollo simulation, while the pedestrian reacted to the real-time behavior of the blue vehicle in our approach.

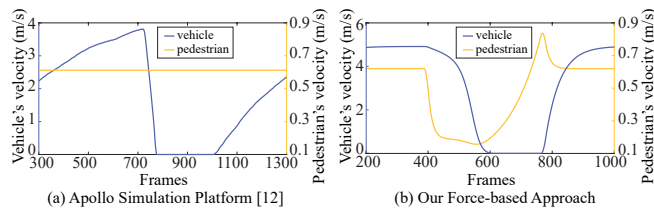


Fig. 6. The comparison of the velocities of both the pedestrian and vehicle between Apollo simulation platform (a) and our approach (b).

road-crossing scenario. We believe our approach can be incorporated into Apollo and Carla simulation platform to simulate pedestrian-vehicle interactions more realistically.

**Bicycle-Vehicle Interactions:** In Fig. 7, we show the snapshots of bicycle-vehicle interactions in two different situations described in Section 3-3.1: (a) a cyclist riding in front of a vehicle; (b) a cyclist riding near the side of a vehicle. For each case, we also show the velocities of both the bicycle and vehicle for comparison. The solid lines represent the velocities in the forward moving direction and the dashed lines indicate those in the lateral direction. As can be seen from Fig. 7, when the bicycle was driving in the near front of the vehicle (from about 430<sup>th</sup> to 530<sup>th</sup> frame), the vehicle decelerated significantly in the forward direction, and its lateral movement did not change significantly. In contrast, when the bicycle was traveling near one side of the vehicle (from about 170<sup>th</sup> to 205<sup>th</sup> frame), the vehicle obviously avoided collision with the bicycle in the lateral direction of movement. At the same time, there was a slight deceleration in the forward moving direction of the vehicle. It is worth noting that in both interaction situations, while the vehicle was reacting, the bicycle also accelerated away from their interaction area and returned to its lane. As depicted in Fig. 7, there was apparent acceleration behavior in both directions of bicycle movement.

## 5. CONCLUSION AND DISCUSSION

In this paper, we devised a virtual mixed-traffic environment that can approximately emulate the intricate urban traffic for autonomous vehicle testing. Pedestrians, bicycles,

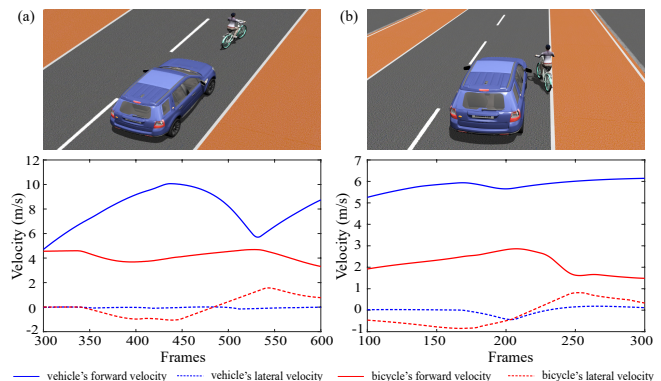


Fig. 7. The snapshots for two kinds of bicycle-vehicle interaction scenarios and the velocities of both the cyclist and vehicle in their interaction process: (a) the cyclist riding in front of the vehicle; (b) the cyclist riding near the side of the vehicle. For the scenario in (a), the vehicle decelerated significantly in the forward moving direction as response to the front bicycle’s movement, while in scenario (b), there is an obvious avoidance behavior in the vehicle’s lateral moving direction to prevent collision with the bicycle by side.

and vehicles are considered as the main road users. Their behaviors are encoded in a general, unified force-based framework, whose forces can be classified as the desire force to a target, the repulsive forces with neighbors and the built environment, and interaction forces between different kinds of road-users. Our approach offers a simple, efficient, and extensible method to simulate different behavioral characteristics of different road users and the realistic interaction effects in complex urban traffic environments. Experimental results have been conducted to validate the performance of our approach by comparing with two popular simulation platforms specifically for autonomous vehicle testing .

Although the simulation results are promising, the approach presented in this paper is still preliminary and can be improved in several aspects. First, the simulation parameters can be set optimally by calibration using real-world traffic data, rather than being set empirically as in the current experiments. Second, it will be more interesting if pedestrians, bicyclists and drivers’ personalized behavioral characteristics can be modeled to generate heterogeneous crowd behaviors, thus generating more versatile and realistic simulations. Third, for pedestrian crossing scenarios, a pedestrian’s decision-making process is far more complex in real-world traffic than that in our current model. Besides the gap acceptance criterion, there are possibly other factors that need to be considered in making the walk-or-wait decisions, such as the total number of pedestrians crossing the road together and the waiting time.

## ACKNOWLEDGMENT

This research project is partially supported by the National Science Foundation (No. 1565978) and an internal grant from HKUST (R9429). Qianwen was supported by Virtual Singapore (No. NRF2015VSGAA3DCM001-014) and the National Natural Science Foundation of China (No. 61702393). Xiaogang Jin was supported by the National Key RD Program of China (No. 2017YFB1002600) and Artificial Intelligence Research Foundation of Baidu Inc.

## REFERENCES

- [1] J. Janai, F. Güney, A. Behl, and A. Geiger, "Computer vision for autonomous vehicles: Problems, datasets and state-of-the-art," *arXiv:1704.05519*, 2017.
- [2] C. Katrakazas, M. Quddus, W.-H. Chen, and L. Deka, "Real-time motion planning methods for autonomous on-road driving: State-of-the-art and future research directions," *Transportation Research Part C: Emerging Technologies*, vol. 60, pp. 416–442, 2015.
- [3] B. Paden, M. Čáp, S. Z. Yong, D. Yershov, and E. Frazzoli, "A survey of motion planning and control techniques for self-driving urban vehicles," *IEEE Transactions on Intelligent Vehicles*, vol. 1, no. 1, pp. 33–55, 2016.
- [4] S. M. Veres, L. Molnar, N. K. Lincoln, and C. P. Morice, "Autonomous vehicle control systemsa review of decision making," *Proceedings of the Institution of Mechanical Engineers, Part I: Journal of Systems and Control Engineering*, vol. 225, no. 2, pp. 155–195, 2011.
- [5] C. C. T. Mendes, V. Frémont, and D. F. Wolf, "Exploiting fully convolutional neural networks for fast road detection," in *IEEE International Conference on Robotics and Automation (ICRA)*, 2016, pp. 3174–3179.
- [6] E. Galceran, A. G. Cunningham, R. M. Eustice, and E. Olson, "Multi-policy decision-making for autonomous driving via changepoint-based behavior prediction," in *Robotics: Science and Systems*, 2015, pp. 2290–2297.
- [7] M. Bojarski, D. Del Testa, D. Dworakowski, B. Firner, B. Flepp, P. Goyal, L. D. Jackel, M. Monfort, U. Muller, J. Zhang, *et al.*, "End to end learning for self-driving cars," *arXiv:1604.07316*, 2016.
- [8] W. Schwarting, J. Alonso-Mora, and D. Rus, "Planning and decision-making for autonomous vehicles," *Annual Review of Control, Robotics, and Autonomous Systems*, vol. 1, pp. 187–210, 2018.
- [9] M. Aeberhard, S. Rauch, M. Bahram, G. Tanzmeister, J. Thomas, Y. Pilat, F. Homm, W. Huber, and N. Kaempchen, "Experience, results and lessons learned from automated driving on germany's highways," *IEEE Intelligent Transportation Systems Magazine*, vol. 7, no. 1, pp. 42–57, 2015.
- [10] S. J. Anderson, S. C. Peters, T. E. Pilutti, and K. Iagnemma, "Design and development of an optimal-control-based framework for trajectory planning, threat assessment, and semi-autonomous control of passenger vehicles in hazard avoidance scenarios," in *Robotics Research*. Springer, 2011, pp. 39–54.
- [11] M. Likhachev and D. Ferguson, "Planning long dynamically feasible maneuvers for autonomous vehicles," *The International Journal of Robotics Research*, vol. 28, no. 8, pp. 933–945, 2009.
- [12] "Apollo simulation," <http://apollo.auto/platform/simulation.html>, 2018.
- [13] A. Best, S. Narang, L. Pasqualin, D. Barber, and D. Manocha, "Autonovi-sim: Autonomous vehicle simulation platform with weather, sensing, and traffic control," in *Neural Information Processing Systems*, 2017.
- [14] A. Dosovitskiy, G. Ros, F. Codevilla, A. Lopez, and V. Koltun, "CARLA: An open urban driving simulator," in *Proceedings of the 1st Annual Conference on Robot Learning*, 2017, pp. 1–16.
- [15] H. Bi, T. Mao, Z. Wang, and Z. Deng, "A data-driven model for lane-changing in traffic simulation," in *Proceedings of the ACM SIGGRAPH/Eurographics Symposium on Computer Animation*, 2016, pp. 149–158.
- [16] J. Shen and X. Jin, "Detailed traffic animation for urban road networks," *Graphical Models*, vol. 74, no. 5, pp. 265–282, 2012.
- [17] Q. Chao, Z. Deng, and X. Jin, "Vehicle–pedestrian interaction for mixed traffic simulation," *Computer Animation and Virtual Worlds*, vol. 26, no. 3–4, pp. 405–412, 2015.
- [18] D. Krajzewicz, J. Erdmann, M. Behrisch, and L. Bieker, "Recent development and applications of SUMO - Simulation of Urban MObility," *International Journal On Advances in Systems and Measurements*, vol. 5, no. 3&4, pp. 128–138, December 2012.
- [19] M. Adnan, F. C. Pereira, C. M. L. Azevedo, K. Basak, M. Lovric, S. Raveau, Y. Zhu, J. Ferreira, C. Zegras, and M. Ben-Akiva, "Sim-mobility: A multi-scale integrated agent-based simulation platform," in *95th Annual Meeting of the Transportation Research Board Forthcoming in Transportation Research Record*, 2016.
- [20] "Vissim," <http://vision-traffic.ptvgroup.com>, 2018.
- [21] D. Helbing and P. Molnar, "Social force model for pedestrian dynamics," *Physical review E*, vol. 51, no. 5, p. 4282, 1995.
- [22] D. Helbing, I. Farkas, and T. Vicsek, "Simulating dynamical features of escape panic," *Nature*, vol. 407, no. 6803, p. 487, 2000.
- [23] A. Alahi, K. Goel, V. Ramanathan, A. Robicquet, L. Fei-Fei, and S. Savarese, "Social lstm: Human trajectory prediction in crowded spaces," in *Proceedings of the IEEE Conference on Computer Vision and Pattern Recognition*, 2016, pp. 961–971.
- [24] A. Cosgun, E. A. Sisbot, and H. I. Christensen, "Anticipatory robot path planning in human environments," in *Robot and Human Interactive Communication (RO-MAN), 2016 25th IEEE International Symposium on*. IEEE, 2016, pp. 562–569.
- [25] D. L. Gerlough, "Simulation of freeway traffic on a general-purpose discrete variable computer," Ph.D. dissertation, University of California, Los Angeles, 1955.
- [26] M. Treiber and D. Helbing, "Microsimulations of freeway traffic including control measures," *at-Automatisierungstechnik*, vol. 49, no. 11, pp. 478–484, 2001.
- [27] A. Kesting and M. Treiber, "Calibrating car-following models by using trajectory data: Methodological study," *Transportation Research Record*, vol. 2088, no. 1, pp. 148–156, 2008.
- [28] A. Kesting, M. Treiber, and D. Helbing, "General lane-changing model mobil for car-following models," *Transportation Research Record: Journal of the Transportation Research Board*, no. 1999, pp. 86–94, 2007.
- [29] B. Wan and N. Roupail, "Using arena for simulation of pedestrian crossing in roundabout areas," *Transportation Research Record: Journal of the Transportation Research Board*, no. 1878, pp. 58–65, 2004.
- [30] P. Koh and Y. Wong, "Gap acceptance of violators at signalised pedestrian crossings," *Accident Analysis & Prevention*, vol. 62, pp. 178–185, 2014.
- [31] S. Kim, S. J. Guy, D. Manocha, and M. C. Lin, "Interactive simulation of dynamic crowd behaviors using general adaptation syndrome theory," in *Proceedings of the ACM SIGGRAPH symposium on interactive 3D graphics and games*, 2012, pp. 55–62.